

Research Article

Rashid Nawaz, Sumera, Laiq Zada, Muhammad Ayaz, Hijaz Ahmad*, Fuad A. Awwad, and Emad A. A. Ismail

Rational approximation for solving Fredholm integro-differential equations by new algorithm

<https://doi.org/10.1515/phys-2022-0181>

received November 07, 2021; accepted March 01, 2023

Abstract: In this article, we used a novel semi-analytical approach, named the optimal auxiliary function method (OAFM), to solve integro-differential equations (IDEs). The OAFM includes an auxiliary function and convergence control parameters, which expedite the convergence of the method. To apply the proposed method, some assumptions regarding small or large parameters in the problem are necessary. We present numerical outcomes acquired *via* the OAFM alongside those obtained from other numerical techniques in tables. Furthermore, we demonstrate the efficacy and ease of implementing the proposed method for various IDEs using 2D graphs.

Keywords: optimal auxiliary function method, exact solutions, Fredholm integro-differential equations

1 Introduction

The integral equations are of utmost importance in various domains of science and technology, with applications ranging from electromagnetics to fluid mechanics. The articles [1,2] highlight the importance of integral equations in

various fields. However, finding exact solutions to non-linear integral equations is a challenging task, and researchers often rely on approximate analytical methods to solve these problems. The development of these methods has enabled scientists and engineers to make significant progress in their respective fields and has led to the discovery of new solutions and phenomena. Therefore, the study of integral equations and their solutions is crucial to advancing our understanding of the natural world and developing new technologies.

A variety of techniques have been developed to solve challenging problems across various scientific and engineering domains. These methods include the Haar function approach [3], the homotopy perturbation method [4,5], the reproducing kernel method [6], the Kudryashov method [7], the modified variational iteration algorithm-II [8–11], the Adomian decomposition method [12], the fixed-point method [13], the use of Genocchi polynomials [14], meshless methods [15–19], the differential transformation technique [20], the Chebyshev wavelets technique [21], the Sinc-collocation method [22], the reproducing kernel Hilbert space methodology [23], and other techniques [24–30]. Each of these methods has its unique advantages and limitations. For instance, perturbation methods are useful for tackling problems with small or large parameters, but they may fail to capture the behavior of the system in the presence of extreme changes. On the other hand, numerical methods provide accurate solutions to complex problems, but they may encounter issues related to discretization. Therefore, it is crucial to select an appropriate artificial parameter assumption when using these methods to solve the equation. The choice of a parameter assumption determines the efficacy and accuracy of the method used to solve the problem. In summary, researchers must weigh the pros and cons of each method carefully and select the most appropriate technique for their specific problem.

Another technique known as the optimal auxiliary function method (OAFM) has been proposed in the same research domain in this study. Unlike perturbation and numerical methods, this method does not require any assumptions regarding small or large parameters or

* **Corresponding author: Hijaz Ahmad**, Operational Research Center in Healthcare, Near East University, Near East Boulevard, PC: 99138 Nicosia/Mersin 10, Turkey; Department of Computer Science and Mathematics, Lebanese American University, Beirut, Lebanon; Section of Mathematics, International Telematic University Uninettuno, Corso Vittorio Emanuele II, 39, Roma 00186, Italy, e-mail: hijaz555@gmail.com, ahmad.hijaz@uninettuno.it

Rashid Nawaz: UniSa STEM, University of South Australia, Adelaide, Australia

Sumera, Laiq Zada, Muhammad Ayaz: Department of Mathematics, Abdul Wali Khan University Mardan Khyber Pakhtunkhwa, Mardan, Pakistan

Fuad A. Awwad, Emad A. A. Ismail: Department of Quantitative analysis, College of Business Administration, King Saud University, P.O. Box 71115, Riyadh 11587, Saudi Arabia

discretization. The approach in the study by Marinca and Herisanu [31] was applied to obtain a series solution for the thin-film flow of a fourth-grade fluid down a vertical cylinder. Subsequently, Zada *et al.* expanded the application of the method to include partial differential equations that pertain to shallow water waves [32]. As a result of the modifications, the technique provides a series solution after just one iteration.

The structure of this article is outlined in the following paragraphs. In Section 2, the recommended method is introduced, along with a discussion of its convergence analysis. Section 3 details the application of this method to various Fredholm integro-differential equations (IDEs), and in Section 4, the numerical and graphical results of OAFM will be showcased.

2 Methodology

To apply the OAFM to solve general IDEs, one can follow the steps outlined in the following [31,32]. Consider the following equation as:

$$F'(\eta) = g(\eta) + \int_a^b K(\eta, \tau)F(\tau)d\tau = 0, \quad F(0) = F_0, \quad (1)$$

where $K(\eta, \tau)$ is the kernel, $g(\eta)$ is a source term, and $F(\eta)$ is an unknown function that can be determined. Similarly, a and b are the lower bound and upper bound of the integral sign.

For the sake of simplicity, we replace some terms in Eq. (1) with the following expression:

- Here, $\frac{d}{d\eta}$ can be replaced by L .
- $\int_a^b K(\eta, \tau)F(\tau)d\tau$ can be replaced by $N(F(\eta))$.

Therefore, Eq. (1) can be expressed in the following manner:

$$L(F(\eta)) = g(\eta) + N(F(\eta)) = 0. \quad (2)$$

Step 1: To obtain a series solution for Eq. (2), we consider a solution that comprises two components in the following form:

$$\tilde{F}(\eta) = F_0(\eta) + F_1(\eta, C_i), \quad i = 1, 2, 3, \dots, p. \quad (3)$$

Step 2: Using OAFM, we can obtain the zero-order and first-order solutions by inserting Eq. (3) into Eq. (2):

$$L(F_0(\eta)) + L(F_1(\eta, C_i)) + g(\eta) + N(F_0(\eta)) = 0. \quad (4)$$

Step 3: The following linear equations can be used to obtain the initial approximation and the first value:

$$L[F_0(\tau) + g(\tau)] = 0, \quad F_0(0) = 0, \quad (5)$$

$$L(F_1(\tau, C_i)) + N(F_0(\tau) + F_1(\tau, C_i)) = 0, \quad F_1(\tau) = 0. \quad (6)$$

Step 4: Therefore, the nonlinear expression in Eq. (6) can be expressed as:

$$N(F_0(\eta) + F_1(\eta, C_i)) = N(F_0(\eta)) + \sum_{k=1}^{\infty} \frac{F_1^k}{k!} (N(F_0(\eta))) \quad (7)$$

Step 5: Upon examining Eq. (7), it becomes apparent that it poses certain difficulties. To address this issue, we explore an alternative expression for Eq. (7) that can be readily solved. Specifically, we consider the following expression:

$$L(F_1(\eta, C_i)) + \Delta_1(F_0(\eta))N(F_0(\eta)) + \Delta_2(F_0(\eta), C_j) = 0, \quad (8)$$

$$F_1(0) = 0.$$

Remark 1. Here, we consider two auxiliary functions, A_1 and A_2 , which are dependent on both the initial approximation $F_0(\eta)$ and a set of unknown parameters C_i and C_j , $i = 1, 2, 3, \dots, j = s + 1, s + 2, \dots, p$.

Remark 2. The auxiliary functions Δ_1 and Δ_2 can take on various forms and may be similar to the form of $F_0(\eta)$, the form of $N[F_0(\eta)]$, or a combination of both $F_0(\eta)$ and $N[F_0(\eta)]$.

Remark 3.

- If either $F_0(\eta)$ or $N(F_0(\eta))$ is a polynomial function, then the auxiliary functions must be the sum of polynomial functions.
- If either $F_0(\eta)$ or $N(F_0(\eta))$ is an exponential function, then the auxiliary functions must be the sum of exponential functions.
- If either $F_0(\eta)$ or $N(F_0(\eta))$ is a trigonometric function, then the auxiliary functions must be the sum of trigonometric functions.
- When $N(F_0(\eta)) = 0$, it can be deduced that $F_0(\eta)$ will be an exact solution for Eq. (4).

Step 7: Various numerical methods have been developed to identify the appropriate values of convergence control parameters C_i . These methods include the least-squares method, collocation method, the Ritz method, and the Galerkin method. In this study, the least-squares method is used to minimize the errors and compute the values of convergence control parameters numerically.

$$J(C_i) = \int_0^1 R^2 d\eta. \quad (9)$$

The symbol “ R ” is used to represent the residual in the following equation:

$$R(\eta, C_i) = \tilde{F}'(\eta) + g(\eta) + N(\tilde{F}(\eta)), \quad i = 1, 2, \dots, n. \quad (10)$$

3 Implementation of OAFM

In this section, we examine the effectiveness of our proposed approach for solving IDEs. To demonstrate the accuracy and efficiency of our method, we present both numerical and graphical results. To simplify the process, we used Mathematica 10 (Figures 1–4).

3.1 Example 1

The linear Fredholm IDE can be expressed as [33]:

$$F'(\eta) + F(\eta) = \frac{1}{2}(e^{-2} - 1) + \int_0^1 F(\tau)^2 d\tau, \quad F(0) = 1. \quad (11)$$

Having exact solution,

$$F(\eta) = e^{-\eta}. \quad (12)$$

The linear and nonlinear terms in Eq. (11) are presented as follows:

$$\begin{aligned} L(F) &= F'(\eta) + F(\eta), \\ N(F) &= -\int_0^1 F(\tau)^2 d\tau, \quad g(\eta) = -\frac{1}{2}(e^{-2} - 1). \end{aligned} \quad (13)$$

The initial approximate $F_0(\eta)$ is obtained from Eq. (5):

$$F'_0(\eta) + F_0(\eta) - \frac{1}{2}(e^{-2} - 1) = 0, \quad F_0(\eta) = 1. \quad (14)$$

The solution for Eq. (14) is written as follows:

$$F_0(\eta) = \frac{1}{2}e^{-2-\eta}(1 - 3e^2 - e^\eta + e^{2+\eta}). \quad (15)$$

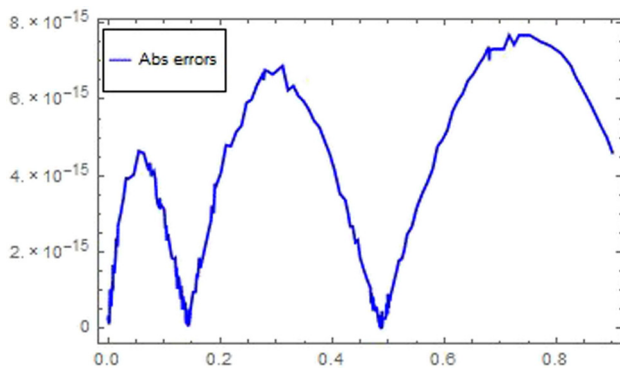


Figure 1: First-order OAFM's absolute error for Problem 1.

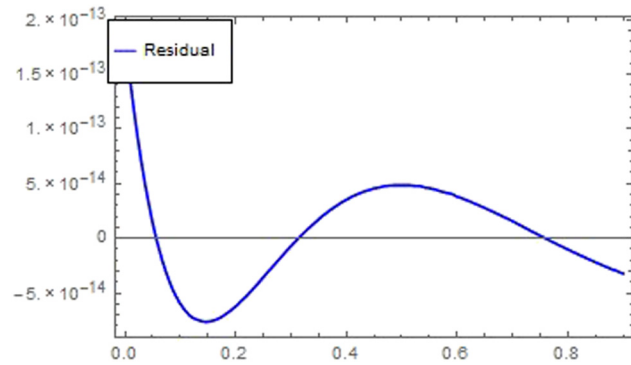


Figure 2: Residual obtained by the first-order OAFM for Problem 1.

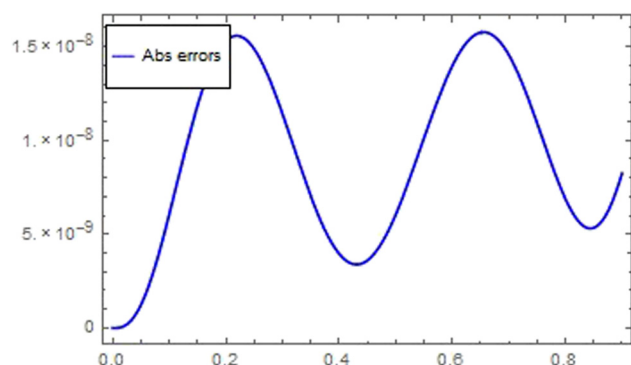


Figure 3: First-order OAFM to calculate the absolute errors for Problem 2.

Upon substituting Eq. (15) into Eq. (13), the nonlinear term is transformed into:

$$N[F_0(\eta)] = -\int_0^1 F_0(\tau)^2 d\tau. \quad (16)$$

Eq. (8) gives the first approximation of $F_1(\eta)$:

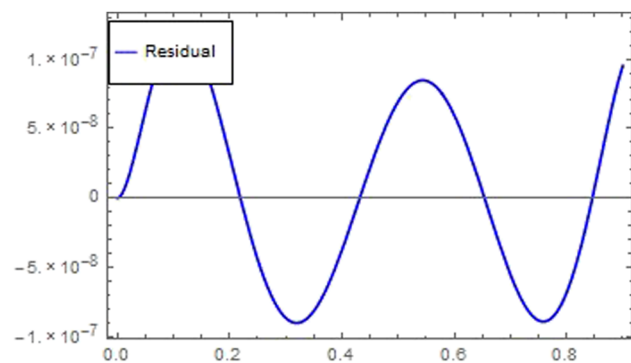


Figure 4: Residual resulting from the application of the first-order OAFM technique to Problem 2.

$$F'_1(\eta) + \Delta_1(F_0(\eta))N[F_0(\eta)] + \Delta_2(F_0(\eta), C_j) = 0, \quad F_1(0) = 0. \quad (17)$$

Based on the properties of the nonlinear operator, the appropriate selections for Δ_1 and Δ_2 are made as follows:

$$\begin{cases} \Delta_1 = C_1(e^{-\eta}) + C_2(\eta e^{-\eta}) + C_3(\eta^2 e^{-2\eta}), \\ \Delta_2 = -C_4(\eta^3 e^{-3\eta}). \end{cases} \quad (18)$$

Substituting Eqs. (15) and (18) into Eq. (17), we obtain the first approximation as:

$$F_1(\eta, C_i) = \begin{bmatrix} 0.2910006975906242e^{-4\eta}(-e^{3\eta}C_1 + e^{4\eta}C_1 \\ - e^{3\eta}C_2 + e^{4\eta}C_2 - e^{3\eta}\eta C_2 \\ - 0.25e^{2\eta}C_3 + 0.25e^{4\eta}C_3 - 0.5e^{2\eta}\eta C_3 \\ - 0.5e^{2\eta}\eta^2 C_3 - 0.2545494725180366e^{\eta}C_4 \\ + 0.2545494725180366e^{4\eta}C_4 \\ - 0.7636484175541097e^{\eta}\eta C_4 \\ - 1.1454726263311648e^{\eta}\eta^2 C_4 \\ - 1.1454726263311645e^{\eta}\eta^3 C_4) \end{bmatrix}. \quad (19)$$

The first-order approximate solution can be obtained by adding Eqs. (15) and (19), resulting in:

$$\tilde{F}(\eta) = F_0(\eta) + F_1(\eta, C_1, C_2, C_3, C_4). \quad (20)$$

In order to determine the values of unknown parameters, we used the least-squares method. The convergence control parameter numerical values pertaining to Problem 1 are displayed in the following. By using these values within

Eq. (20), we obtained an approximate solution of first-order (Tables 1–3):

$$C_1 = 1.4856746460109285, \quad C_2 = -1.6556793446784177 \times 10^{-11}, \\ C_3 = 9.956020463982691 \times 10^{-11}, \\ \text{and } C_4 = -4.547365481306824 \times 10^{-11}.$$

3.2 Problem 2

The linear Fredholm IDE can be represented as [33]:

$$F'(\eta) = \eta^2(2e^{-1} - 1) - e^{-\eta} + \int_0^1 (\eta^2 \tau) F(\tau) d\tau, \quad F(0) = 1. \quad (21)$$

Having exact solution,

$$F(\eta) = e^{-\eta}. \quad (22)$$

The linear and nonlinear terms for Eq. (21) are provided in the following:

$$L(F) = F'(\eta), \quad N(F) = -\int_0^1 (\eta^2 \tau) F(\tau) d\tau, \quad (23)$$

$$g(\eta) = -\eta^2(2e^{-1} - 1) + e^{-\eta}.$$

To obtain the initial approximation $F_0(\eta)$, Eq. (5) is used:

$$F'_0(\eta) - \eta^2(2e^{-1} - 1) + e^{-\eta} = 0, \quad F_0(0) = 1. \quad (24)$$

The solution to Eq. (24) can be expressed as:

Table 1: In Problem 1, the first-order solution of the OAFM is compared with the exact solution, and the absolute errors from the OAFM are compared with those of the semi-orthogonal B-spline wavelets method, with varying values of η

| η | OHAM solution | Exact solution | Kernel Hilbert space method [33] | Absolute error OAFM |
|--------|---------------|----------------|----------------------------------|---------------------------|
| 0.16 | 0.852144 | 0.852144 | 5.51442×10^{-7} | 1.52656×10^{-15} |
| 0.32 | 0.726149 | 0.726149 | 8.40507×10^{-7} | 6.20337×10^{-15} |
| 0.48 | 0.618783 | 0.618783 | 1.14152×10^{-6} | 2.498×10^{-16} |
| 0.64 | 0.527292 | 0.527292 | 7.78753×10^{-6} | 6.30052×10^{-15} |
| 0.8 | 0.449329 | 0.449329 | 8.17887×10^{-6} | 7.35523×10^{-15} |
| 0.96 | 0.382893 | 0.382893 | 1.29618×10^{-5} | 2.33147×10^{-15} |

Table 2: In Problem 2, the accuracy of the OAFM is evaluated by comparing its first-order solution with the exact solution. Furthermore, the absolute errors obtained from the OAFM are compared with those from the kernel Hilbert space method, while varying a parameter η

| η | OAFM solution | Exact solution | Kernel Hilbert space method [33] | Absolute error OAFM |
|--------|---------------|----------------|----------------------------------|--------------------------|
| 0.16 | 0.852144 | 0.852144 | 1.61428×10^{-8} | 1.28272×10^{-8} |
| 0.32 | 0.726149 | 0.726149 | 3.04839×10^{-8} | 9.64626×10^{-9} |
| 0.48 | 0.618783 | 0.618783 | 4.33347×10^{-8} | 4.7838×10^{-9} |
| 0.64 | 0.527292 | 0.527292 | 5.49647×10^{-8} | 1.56199×10^{-8} |
| 0.8 | 0.449329 | 0.449329 | 6.56068×10^{-8} | 6.8857×10^{-9} |
| 0.96 | 0.382893 | 0.382893 | 7.54625×10^{-8} | 1.42266×10^{-8} |

$$F_0(\eta) = e^{-\eta} - \frac{\eta^3}{3} + \frac{2\eta^3}{3e}. \quad (25)$$

By inserting Eq. (25) into Eq. (23), the nonlinear component is transformed into:

$$N[F_0(\eta)] = -\int_0^1 (\eta^2 \tau) F_0(\tau) d\tau. \quad (26)$$

Eq. (8) provides the initial estimate or first approximation $F_1(\eta)$:

$$\begin{aligned} F_1'(\eta) + \Delta_1(F_0(\eta))N[F_0(\eta)] + \Delta_2(F_0(\eta), C_j) \\ = 0, \quad F_1(0) = 0. \end{aligned} \quad (27)$$

Choosing Δ_1 and Δ_2 , based on the nonlinear operator,

$$\begin{cases} \Delta_1 = C_1(e^{-\eta}) + C_2(\eta e^{-\eta}) + C_3(\eta^2 e^{-\eta}) + C_4(\eta^3 e^{-\eta}) \\ \quad + C_5(\eta^4 e^{-\eta}), \\ \Delta_2 = -C_6(\eta^3). \end{cases} \quad (28)$$

Using Eqs. (25) and (28) into Eq. (27), we obtain the first approximation as:

$$F_1(\eta, C_i) = \begin{bmatrix} -0.246625043146641e^{-\eta}(2C_1 + 6C_2 + 24C_3 \\ + 120C_4 + 720C_5 - 2C_1e^{\eta} \\ - 6.000000000000001C_2e^{\eta} - 24C_3e^{\eta} \\ - 120C_4e^{\eta} - 720C_5e^{\eta} + 2C_1\eta \\ + 6C_2\eta + 24C_3\eta + 120C_4\eta + 720C_5\eta + C_1\eta^2 \\ + 3C_2\eta^2 + 12C_3\eta^2 + 60C_4 \\ \eta^2 + 360C_5\eta^2 + C_2\eta^3 + 4C_3\eta^3 + 20C_4\eta^3 \\ + 120C_5\eta^3 + C_3\eta^4 + 5C_4\eta^4 \\ + 30C_5\eta^4 - 1.0136845667021426C_6e^{\eta}\eta^4 \\ + C_4\eta^5 + 6C_5\eta^5 + C_5\eta^6) \end{bmatrix}. \quad (29)$$

The first-order approximate solution can be obtained by adding Eqs. (25) and (29), resulting in:

$$\tilde{F}(\eta) = F_0(\eta) + F_1(\eta, C_1, C_2, C_3, C_4, C_5, C_6). \quad (30)$$

To compute the unknown parameters, we used the least-squares method. The convergence control parameters were obtained using numerical values:

$$\begin{aligned} C_1 &= 1.0716181266089877, & C_2 &= 0.9236853396995555, \\ C_3 &= 0.39757730004729536, & C_4 &= 0.09242573846085574, \\ C_5 &= 0.030962705288356332, & \text{and } C_6 &= 0.03594407264216984. \end{aligned}$$

The first-order approximate solution for Problem 2 can be obtained by applying the values to Eq. (30).

3.3 Problem 3

The nonlinear Fredholm IDE [33] is as follows:

$$\begin{aligned} F'''(\eta) &= \sin(\eta) - \eta - \int_0^{\frac{\pi}{2}} \eta \tau F'(\tau) d\tau, \\ F(0) &= 1, F'(0) = 0, \text{ and } F''(0) = -1. \end{aligned} \quad (31)$$

Having exact solution,

$$F(\eta) = \cos(\eta). \quad (32)$$

The linear and nonlinear terms in Eq. (31) are presented as follows:

$$\begin{cases} L(F) = F'''(\eta), \\ N(F) = -\sin(\eta) + \int_0^{\frac{\pi}{2}} \eta \tau F'(\tau) d\tau, \\ g(\eta) = \eta. \end{cases} \quad (33)$$

We obtain the initial approximation $F_0(\eta)$ from Eq. (5):

Table 3: Comparative analysis of the first-order OAFM solution with the exact as well as with the semi-orthogonal spline wavelet method with the variation of η for Problem 3

| η | OAFM solution | Exact solution | Method in [34] | Absolute error OAFM |
|--------|---------------|----------------|-----------------------------|--------------------------|
| 0.0 | 1. | 1. | 0.0 | 0. |
| 0.1 | 0.995043 | 0.995004 | 0.0 | 3.84199×10^{-5} |
| 0.2 | 0.980308 | 0.980067 | $4.63105000 \times 10^{-4}$ | 2.41174×10^{-4} |
| 0.3 | 0.95593 | 0.955336 | $1.42980700 \times 10^{-3}$ | 5.93344×10^{-4} |
| 0.4 | 0.921954 | 0.921061 | $2.94384300 \times 10^{-3}$ | 8.93085×10^{-4} |
| 0.5 | 0.878348 | 0.877583 | $5.05241100 \times 10^{-3}$ | 7.6591×10^{-4} |
| 0.6 | 0.825019 | 0.825336 | $7.80640100 \times 10^{-3}$ | 3.16757×10^{-4} |
| 0.7 | 0.761826 | 0.764842 | $1.12606240 \times 10^{-2}$ | 3.01612×10^{-3} |
| 0.8 | 0.688603 | 0.696707 | $1.54740510 \times 10^{-2}$ | 8.10341×10^{-3} |
| 0.9 | 0.605172 | 0.62161 | $2.05100590 \times 10^{-2}$ | 1.6438×10^{-2} |
| 1.0 | 0.511353 | 0.540302 | $2.64366750 \times 10^{-2}$ | 2.8949×10^{-2} |

$$F_0'''(\eta) + \eta = 0, \quad F_0(0) = 1, \quad F_0'(0) = 0, \quad F_0''(0) = -1. \quad (34)$$

The solution for Eq. (34) is written as follows:

$$F_0(\eta) = \frac{1}{24}(24 - 12\eta^2 - \eta^4). \quad (35)$$

The nonlinear term can be expressed by inserting Eq. (35) into Eq. (33):

$$N(F) = -\sin(\eta) + \int_0^{\frac{\pi}{2}} \eta \tau F'(\tau) d\tau. \quad (36)$$

Eq. (8) provides an initial approximation $F_1(\eta)$:

$$F_1'''(\eta) + \Delta_1(F_0(\eta))N[F_0(\eta)] + \Delta_2(F_0(\eta), C_j) = 0, \quad (37)$$

$$F_1(0) = 1, \quad F_1'(0) = 0, \quad F_1''(0) = 0.$$

Choosing Δ_1 and Δ_2 , based on the nonlinear operator,

$$\begin{cases} \Delta_1 = C_1(\eta^2) + C_2(\eta^4), \\ \Delta_2 = -C_3. \end{cases} \quad (38)$$

Using Eqs (35) and (38) into Eq. (37), we obtain the first approximation as:

$$F_1(\eta) = \left\{ \begin{aligned} &0.013422489166643006(894.0219545732162C_1 \\ &- 74.50182954776801\eta^2C_1 \\ &+ \eta^6C_1 - 894.0219545732162 \cos(\eta)C_1 \\ &+ 74.50182954776801\eta^2 \cos(\eta)C_1 \\ &- 447.0109772866081\eta \sin(\eta)C_1 \\ &- 26820.658637196488C_2 \\ &+ 894.0219545732141\eta^2C_2 \\ &+ 0.3571428571428571\eta^8C_2 \\ &+ 26820.658637196488 \cos(\eta)C_2 \\ &- 5364.131727439297\eta^2 \cos(\eta)C_2 \\ &+ 74.50182954776801\eta^4 \cos(\eta)C_2 \\ &+ 17880.439091464326\eta \sin(\eta)C_2 \\ &- 894.0219545732162\eta^3 \sin(\eta)C_2 \\ &+ 12.416971591294667\eta^3C_3). \end{aligned} \right. \quad (39)$$

The first-order approximate solution can be obtained by adding Eqs. (35) and (39), resulting in:

$$\tilde{F}(\eta) = F_0(\eta) + F_1(\eta, C_1, C_2, C_3). \quad (40)$$

To compute the unknown parameters, we used the least-squares method. The convergence control parameters were then obtained numerically:

$$C_1 = 0.33393443948168094, \quad C_2 = -0.10972453346288534, \\ \text{and } C_3 = 0.28046744091671133.$$

The initial solution of the first-order approximation can be obtained by applying the values to Eq. (40).

4 Conclusion

The OAFM technique is used to address IDEs, including those belonging to the family of IDEs. The numerical results are compared with those obtained by the kernel Hilbert space and other numerical methods used in the literature. Based on the numerical and graphical findings, it can be stated that the suggested approach offers several benefits. First, the method is simple to execute and delivers an approximate solution in a single iteration. Additionally, the method comprises convergence control parameters and auxiliary functions that regulate its convergence. There is no requirement for assumptions regarding small or large parameters in the equation being solved. Furthermore, enhancing the precision of the method is achievable by increasing the number of convergence control parameters. Based on the evidence presented, it appears that the method used in this study is highly efficient and could potentially be applied to address other complex, nonlinear problems encountered in various scientific and technological domains.

Acknowledgments: The authors acknowledge Researchers Supporting Project Number (RSPD2023R576), King Saud University, Riyadh, Saudi Arabia.

Funding information: This project was funded by King Saud University, Riyadh, Saudi Arabia.

Author contributions: All authors have accepted responsibility for the entire content of this manuscript and approved its submission.

Conflict of interest: The authors state no conflict of interest.

References

- [1] Yüzbaşı Ş, Şahin N, Sezer M. Numerical solutions of systems of linear Fredholm integro differential equations with Bessel polynomial bases. *Comput Math Appl*. 2011;61(10):3079–96.
- [2] Maleknejad K, Torabi P, Sauter S. Numerical solution of a non-linear Volterra integral equation. *Vietnam J Math*. 2016;44(1):5–28.
- [3] Liu X, Ahsan M, Ahmad M, Nisar M, Liu X, Ahmad I, et al. Applications of Haar wavelet-finite difference hybrid method and its convergence for hyperbolic nonlinear Schrödinger equation with energy and mass conversion. *Energies*. 2021;14(23):7831.

- [4] Hasan PM, Sulaiman NA. Convergence analysis for the homotopy perturbation method for a linear system of mixed Volterra-Fredholm integral equations. *Baghdad Sci J*. 2020;17(3 Suppl):1010.
- [5] Shah NA, Ahmad I, Omar B, Abouelregal AE, Ahmad H. Multistage optimal homotopy asymptotic method for the nonlinear Riccati ordinary differential equation in nonlinear physics. *Appl Math Inf Sci*. 2020;14(6):1–7.
- [6] Akgül A, Ahmad H. Reproducing kernel method for Fangzhu's oscillator for water collection from air. *Math Methods Appl Sci*. 2020. doi: 10.1002/mma.6853.
- [7] Yusuf A, Sulaiman TA, Khalil EM, Bayram M, Ahmad H. Construction of multi-wave complexiton solutions of the Kadomtsev-Petviashvili equation *via* two efficient analyzing techniques. *Results Phys*. 2020;21:103775.
- [8] Ahmad H, Akgül A, Khan TA, Stanimirović PS, Chu Y-M. New perspective on the conventional solutions of the nonlinear time-fractional partial differential equations. *Complexity*. 2020;2020:8829017. doi: 10.1155/2020/8829017.
- [9] Ahmad H, Khan TA, Ahmad I, Stanimirović PS, Chu Y-M. A new analyzing technique for nonlinear time fractional Cauchy reaction-diffusion model equations. *Results Phys*. 2020;19:103462.
- [10] Ahmad H, Khan TA, Yao SW. An efficient approach for the numerical solution of fifth-order KdV equations. *Open Math*. 2020;18(1):738–48.
- [11] Ahmad H, Khan TA. Variational iteration algorithm I with an auxiliary parameter for the solution of differential equations of motion for simple and damped mass-spring systems. *Noise Vib Worldw*. 2020;51(1–2):12–20.
- [12] Khanian M, Davari A. Solution of system of Fredholm integro-differential equations by Adomian decomposition method. *Aust J Basic Appl Sci*. 2011;5(12):2356–61.
- [13] Berenguer MI, Gámez D, López Linares AJ. Solution of systems of integro-differential equations using numerical treatment of fixed point. *J Comput Appl Math*. 2017;315:343–53.
- [14] Loh JR, Phang C. A new numerical scheme for solving system of Volterra integro-differential equation. *Alex Eng J*. 2018;57(2):1117–24.
- [15] Khan MN, Ahmad I, Akgül A, Ahmad H, Thounthong P. Numerical solution of time-fractional coupled Korteweg-de Vries and Klein-Gordon equations by local meshless method. *Pramana-J Phys*. 2021;95(1):1–3.
- [16] Ahmad I, Ahmad H, Inc M, Yao S-W, Almohsen B. Application of local meshless method for the solution of two term time fractional-order multi-dimensional PDE arising in heat and mass transfer. *Therm Sci*. 2020;24:95–105.
- [17] Nawaz M, Ahmad I, Ahmad H. A radial basis function collocation method for space-dependent inverse heat problems. *J Appl Comput Mech*. 2020;6(SI):1187–99.
- [18] Ali SN, Ahmad I, Abu-Zinadah H, Mohamed KK, Ahmad H. Multistage optimal homotopy asymptotic method for the K (2, 2) equation arising in solitary waves theory. *Therm Sci*. 2021;25(Spec. issue 2):199–205.
- [19] Wang FZ, Hou ER, Ahmad I, Ahmad H. An efficient meshless method for hyperbolic telegraph equations. *CMES-Comput Model Eng Sci*. 2021;128(2):687–98.
- [20] Yüzbaşı Ş, Ismailov N. Solving systems of Volterra integral and integrodifferential equations with proportional delays by differential transformation method. *J Math*. 2014;2014:725648.
- [21] Biazar J, Ebrahimi H. A strong method for solving systems of integro-differential equations. *Appl Math*. 2011;2(9):1105–13. doi: 10.4236/am.2011.29149.
- [22] Hesameddini E, Asadolahifard E. Solving systems of linear Volterra integro-differential equations by using Sinc-collocation method. *Int J Math Eng Sci*. 2013;2(7):1–9.
- [23] Al-Smadi M, Altawallbeh Z. Solution of a system of Fredholm integro-differential equations by RKHS method. *Int J Contemp Math Sci*. 2013;8(11):531–40.
- [24] Muhammad T, Ahmad H, Farooq U, Akgül A. Computational investigation of magnetohydrodynamics boundary of Maxwell fluid across nanoparticle-filled sheet. *Al-Salam J Eng Technol*. 2023;2(2):88–97. doi: 10.55145/ajest.2023.02.02.011.
- [25] Hussain A, Arshad M, Rehman A, Hassan A, Elagan SK, Ahmad H, et al. Three-dimensional water-based magneto-hydrodynamic rotating nanofluid flow over a linear extending sheet and heat transport analysis: A numerical approach. *Energies*. 2021;14(16):5133.
- [26] Tariq M, Ahmad H, Cesarano C, Abu-Zinadah H, Abouelregal AE, Askar S. Novel analysis of hermite-hadamard type integral inequalities *via* generalized exponential type m-convex functions. *Mathematics*. 2022;10(1):31.
- [27] Mohammed WW, Ahmad H, Boulares H, Khelifi F, El-Morshedy M. Exact solutions of Hirota-Maccari system forced by multiplicative noise in the Itô sense. *J Low Freq Noise Vib Active Control*. 2021;41(1):74–84.
- [28] Ahmad I, Ahmad H, Inc I. Performance of meshless method of lines for the solution of the generalized seventh-order Korteweg-de Vries equation having applications in fluid mechanics. *Therm Sci*. 2022;27(Spec. issue 1):S383–8.
- [29] Ahmad I, Ahmad H, Inc I, Rezazadeh H, Akbar MA, Khater MMA, et al. Solution of fractional order Korteweg-de Vries and Burgers' equations utilizing local meshless method. *J Ocean Eng Sci*. 2021. doi: 10.1016/j.joes.2021.08.014.
- [30] Wang F, Zheng K, Ahmad I, Ahmad H. Gaussian radial basis functions method for linear and nonlinear convection-diffusion models in physical phenomena. *Open Phys*. 2021;19(1):69–76.
- [31] Marinca V, Herisanu N. Optimal auxiliary functions method for the thin-film flow of a fourth-grade fluid down a vertical cylinder. *Rom J Tech Sci Appl Mech*. 2017;62(2):181–9.
- [32] Zada L, Khan I, Khan M, Khan A. New algorithm for the approximate solution of generalized seventh order Korteweg-Devries equation arising in shallow water waves. *Results Phys*. 2019;20:103744.
- [33] Arqub OA, Al-Smadi M, Shawagfeh N. Solving Fredholm integro-differential equations using reproducing kernel Hilbert space method. *Appl Math Comput*. 2013;219(17):8938–48.
- [34] Darania P, Ebadian A. A method for the numerical solution of the integro-differential equations. *Appl Math Comput*. 2007;188(1):657–68.